Geohazard Mechanics 4 (2026) 21–28

Contents lists available at ScienceDirect

Geohazard Mechanics

journal homepage: www.keaipublishing.com/en/journals/geohazard-mechanics

Rockburst failure characteristics of sandstone under true triaxial double-sided rapid unloading conditions under high pressure

Jieyu Li[a], Pengfei Shan[a], Jianning Liu[b,*], Yunpeng Guo[c], Xiaomin Wang[a], Zihan Feng[d], Chenguang Liu[e], Chaochao Tian[f], Yuting Mao[c,g]

[a] College of Energy Science and Engineering, Xi'an University of Science and Technology, Xi'an 710054, China
[b] School of Resource and Safety Engineering, University of Science and Technology, Beijing 100083, China
[c] State Key Laboratory for Tunnel Engineering, China University of Mining and Technology (Beijing), Beijing 100083, China
[d] Shuanglong Coal Mine, Huangling Mining, Shaanxi Coal Group, Huangling 727300, China
[e] China Coal Technology Engineering Group Xi'an Research Insititute, Xi'an 710000, China
[f] Ruineng Coal Mine, Huangling Mining, Shaanxi Coal Group, Huangling 727300, China
[g] Department of Civil and Environmental Engineering, University of Alberta, Edmonton 51063, Canada

ARTICLE INFO

Keywords:
True triaxial
Double free surface rockburst
Ejection velocity
Acoustic emission
Crack evolution

ABSTRACT

To explore the evolution process and failure characteristics of rockburst in rock masses with a double free surface structure, we conducted a comparative study between true triaxial double-face rapid unloading rockburst tests and single-face rapid unloading rockburst tests, using a true triaxial experimental system capable of rapid unloading from multiple faces. The main conclusions are as follows: the maximum ejection velocity of double-free surface rockburst fragments is higher than that of single-free surface rockburst (20 %–40 %), and the rockburst ejection duration is generally longer than that of single-free surface rockburst; the peak stress of double-free surface rockburst is smaller than that of single-free surface rockburst, but there will be a more obvious unloading platform stage during unloading. Compared with single-surface unloading rockburst, double-surface unloading is more likely to cause significant brittle failure and violent rockburst; the AE events of single-free surface rockburst are concentrated near one free surface, while the AE events of double-free surface experiments are distributed near two free surfaces. In the later stage of both rockburst experiments, the number of shear cracks will exceed that of tensile cracks. The extra free surface of double-free surface rockburst will enhance crack extension, especially shear cracks, resulting in more serious rock damage.

1. Introduction

Rockbursts and coalbursts are common dynamic disaster phenomena in deep rock mass engineering, closely associated with the rapid release of high elastic strain energy stored within the rock mass [1,2]. In recent years, with the continuous development of underground engineering in deep-buried rock masses, the problem of rockbursts has become increasingly prominent, emerging as a critical research focus in the field of rock mechanics and engineering [3,4]. Consequently, rockburst in deep rock mass engineering has become a pressing and challenging issue in rock mechanics and a significant scientific and technological problem requiring urgent resolution [5]. Moreover, deep underground engineering often contains a large number of double-free-face rock mass structures. For instance, the sidewalls of tunnels or roadways, and the roof and sidewalls of underground caverns in hydropower stations typically form double-free-face rock configurations. Under high-stress conditions, these structures may result in stronger stress concentrations, thereby increasing the likelihood of triggering rockburst disasters.

Since 2006, He et al. first reproduced the dynamic rockburst failure phenomenon in a laboratory setting using a self-developed true triaxial experimental system capable of rapid unloading, and true triaxial rockburst simulation experiments have gradually become an essential tool for studying rockburst mechanisms [6,7]. Selahattin [8] used this experimental system to investigate the influence of thermal damage on strainbursts, calculating the ejection kinetic energy from the rockburst debris velocity on the free face of granite specimens. The study revealed

* Corresponding author.
E-mail address: liujianning617@163.com (J. Liu).
Peer review under the responsibility of Liaoning University.

https://doi.org/10.1016/j.ghm.2026.01.004
Received 18 April 2025; Received in revised form 15 August 2025; Accepted 7 January 2026
Available online 8 January 2026

that rockburst intensity first decreased and then increased with growing thermal damage. Su et al. [9] utilized a self-developed true triaxial rockburst system capable of one-sided rapid unloading to monitor acoustic signals during the rockburst process, analyzed the sound signal indicators related to brittle failure in different rock types, and proposed an intensity evaluation index for rockbursts based on acoustic signals. Wang et al. [10] conducted true triaxial single-sided unloading rockburst experiments and used moment tensor inversion to analyze fracture distribution. Ren et al. explored the relationship between internal coal temperature, stress, and fractures, and derived an equation describing stress-induced temperature changes, validated using thermodynamic parameters. Ren et al. [11] conducted borehole unloading experiments in coal samples to investigate the effectiveness of different borehole types in rockburst prevention and control. Liu et al. [12] performed true triaxial one-sided unloading tests on granite specimens with various borehole configurations, analyzing the rockburst prevention mechanism and the influence of borehole number on rockburst intensity from both mechanical behavior and energy evolution perspectives. Li et al. [13] conducted true triaxial one-sided rapid unloading experiments, studied the critical AE characteristics during the rockburst process, and identified precursory signals based on the critical slowing-down theory. To explore the influence law and mechanism of different bedding inclinations on impact rockburst, Liu et al. [14] used the self-developed true triaxial impact rockburst test equipment to conduct a series of impact rockburst tests on sandstone specimens with five different bedding inclinations. The test process was monitored and recorded in real time using a micro camera device and an AE monitoring system. Qian et al. [15] adopted a physical simulation method for spontaneous rockbursts, developed a multi-source information monitoring system with millisecond resolution to capture the transient dynamic behavior of rockbursts, analyzed the instantaneous static-dynamic transition process, and explored the spontaneous mutation mechanism of rockbursts from the perspectives of mechanics and energy. The above studies have conducted a substantial amount of meaningful research on simulating single free surface rockbursts using true triaxial experiments. However, experimental investigations on rockbursts involving dual free surfaces remain relatively limited. This is particularly noteworthy given the increasing prevalence of dual free surface rock mass structures in deep underground engineering, such as at tunnel intersections, exposed ends, arch-wall junctions, and chamber separation zones. Given the increasing prevalence of double-free-face rock structures in underground rock engineering, it is imperative to conduct systematic experimental investigations to explore their failure characteristics and catastrophic evolution processes.

Firstly, this study conducted true triaxial rockburst simulation experiments under single-sided and double-sided rapid unloading conditions based on the actual stress transition paths of surrounding rock units in deep rock masses, then analyzed the failure characteristics and ejection velocities of rockbursts under double-free-face conditions, subsequently compared the stress–strain responses of single-free-face and double-free-face rockbursts, finally, explored the AE localization patterns and fracture evolution characteristics under both structural conditions. This research provides a scientific basis for the support design of dual free surface rock mass structures, the optimization of pressure relief schemes, and the deployment of multi-point monitoring systems, aiming to achieve early warning and effective control in high-risk areas.

2. Experimental procedures

2.1. Experimental equipment and samples

The experimental setup employed a true triaxial rockburst simulation apparatus capable of independently applying three principal stresses and precisely controlling complex stress paths, as shown in Fig. 1a. The core structure comprises three orthogonally arranged servo-controlled hydraulic loading systems, including a high-stiffness frame,

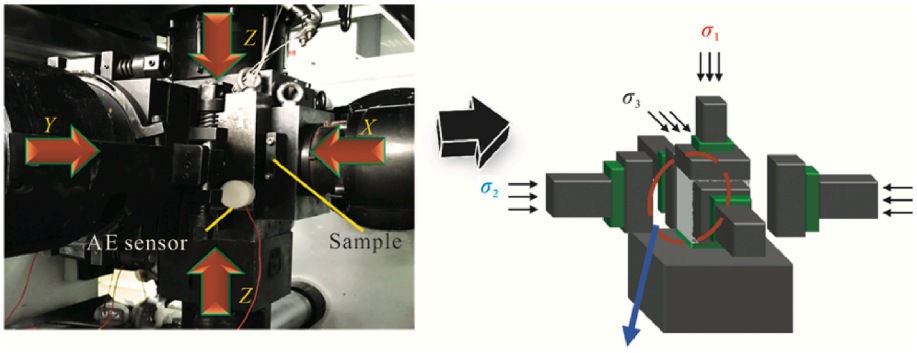

(a) True triaxial equipment (b) Double-sided unloading

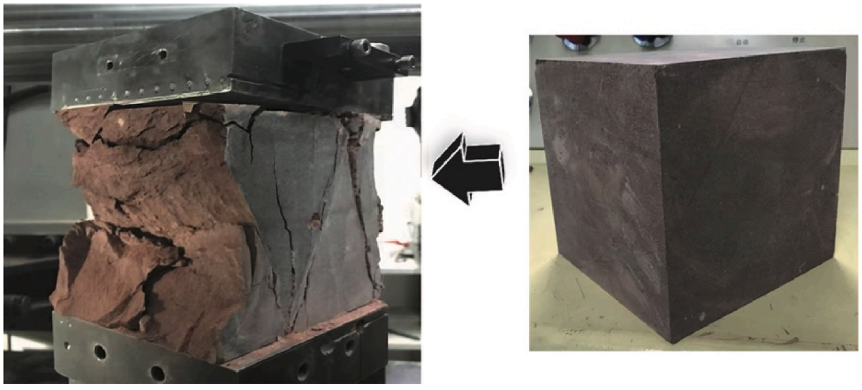

(c) Sample after rock burst (d) Sample

Fig. 1. True triaxial test equipment and sandstone specimens.

three-directional independent loading actuators, and a rapid dual-free-face unloading device. In the rockburst unloading experiment, the maximum unloading rate of this system can reach 200 MPa/s.

During the true triaxial rockburst simulation tests, the sample is subjected to full triaxial confinement up to the initial in-situ stress level. Subsequently, a rapid unloading is applied in the *Y* direction to create dual free surfaces, thereby simulating the excavation-induced dual-free-face rock mass structure, as illustrated in Fig. 1b. Standard cubic sandstone specimens with dimensions of 150 mm were used, with dimensional tolerances controlled within ±0.3 mm through precision cutting, as shown in Fig. 1c. The uniaxial compressive strength of the sandstone cylindrical specimen is about 90 MPa, the elastic modulus is 56 GPa, and the Poisson's ratio is about 0.12, which is a high-strength homogeneous sandstone. Fig. 1d presents a post-failure photograph of a specimen subjected to dual-free-face rockburst testing. During specimen installation, the parallelism between the three loading plates and the specimen surfaces was carefully maintained. A high-speed camera was positioned on the free face side to capture real-time surface damage evolution during the rockburst process. In addition, the experimental system was equipped with a PAC Micro-II acoustic emission monitoring system, featuring a maximum sampling rate of 40 Msps and Nano-30 sensors for signal acquisition.

2.2. Experimental simulation method and loading path

Prior to excavation, deep intact rock is typically subjected to a three-dimensional stress state. After excavation, the creation of one or two free surfaces results in a redistribution of the surrounding rock stress. The tangential stress around the newly formed free surface increases, while the radial stress diminishes and eventually drops to zero. When the concentrated tangential stress exceeds the strength of the rock, a rockburst is triggered. Fig. 2 illustrates the loading paths of true triaxial rockburst simulation tests for rock masses with single and double free surfaces.

Initially, all three principal stresses are simultaneously applied to simulate the in-situ stress conditions of the original rock ($\sigma_1 = 120$ MPa, $\sigma_2 = 60$ MPa, and $\sigma_3 = 30$ MPa). After holding the load for a period to ensure stress stabilization within the rock specimen, σ_3 is rapidly unloaded to simulate excavation-induced stress release. For the double free surface rockburst simulation, both loading forces in the σ_3 direction are unloaded simultaneously. For the single free surface case, only one loading force (σ_{31}) is rapidly unloaded while the other (σ_{32}) is maintained at a nearly zero but stable value. Following unloading, σ_2 remains constant, and σ_1 is subsequently increased to simulate stress concentration until rockburst occurs. In this study, two sets of experiments were conducted: single-sided unloading rockburst experiments and double-sided unloading rockburst experiments, with three tests performed in each set. The simulations of single and dual free surface rockbursts were carried out under stress-controlled loading, with a loading rate of 2 kN/s.

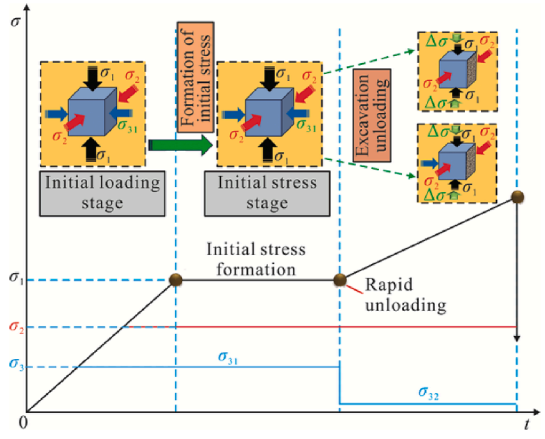

Fig. 2. True triaxial single free surface and double free surface rock burst loading paths.

3. Experimental results and analysis

3.1. Rockburst damage characteristics and ejection speed

High-speed imaging technology was employed to observe the dynamic failure characteristics of rockburst under double free surface conditions, with a frame rate of 1000 frames per second (fps). Fig. 3 presents a typical ejection failure process of rockburst induced by double-surface unloading. Each specimen contains two free surfaces, denoted as free surface 1 and free surface 2. The numbers shown below each image indicate the corresponding time of the observed phenomena, expressed in the format h:m:s:ms (hour:minute:second:millisecond). As shown in Fig. 3, due to the anisotropic nature of the rock, the ejection processes at the two free surfaces are not completely identical, and there exists a time lag between the occurrences of full-scale spalling. The trajectories of the rockburst fragments exhibit a downward parabolic path, and the fragments are predominantly laminar in shape.

To quantify the ejective velocity of rockburst fragments in both experimental conditions, the particle image velocimetry (PIV) technique, commonly used in flow field characterization, was applied to measure the fragment ejection velocities [16]. The variation curves of the average surface velocity for single-surface and double-surface unloading rockburst events are shown in Fig. 4. As illustrated, under both single and double free surface conditions, the ejective velocity exhibits a general trend of gradual increase followed by attenuation. However, the peak velocity and duration of ejection under double free surface conditions are significantly higher than those under single surface conditions.

Specifically, in the double free surface scenario (black and red curves), a relatively small initial velocity peak appears, followed by a more pronounced peak occurring around 100–200 ms, with maximum velocities exceeding 4 m/s. Additionally, the attenuation phase lasts longer. In contrast, the single free surface condition (blue curve) shows a lower peak velocity (generally below 3 m/s) and an earlier onset of decay. Statistics on the maximum ejection velocities of the two groups of rockburst experiments showed that the maximum ejection velocity of double-free rockburst was 20 %–40 % higher than that of single-sided rockburst. These results indicate that the presence of two free surfaces enhances and prolongs the kinetic energy release during the rockburst process, resulting in higher surface ejection velocities and extended duration.

3.2. Stress-strain response characteristics

The stress–strain curves obtained from the two types of rockburst experiments (Fig. 5) reveal that both single-free-face and double-free-face rockbursts exhibit a distinct sequence of mechanical responses, including an initial compaction stage of pre-existing microcracks, an elastic deformation stage, a rapid unloading plateau, a yield stage, and a post-peak stress drop stage. During the elastic deformation stage, both the single-free-face (black curve) and double-free-face (blue curve) rockbursts show a similar increasing trend. However, the single-free-face rockburst reaches a higher peak stress of approximately 190 MPa. In contrast, the double-free-face specimens exhibit a slightly lower maximum stress of around 180 MPa, yet demonstrate a more pronounced unloading plateau during the unloading phase.

As shown in Fig. 5, the elastic energy stored within the rock under dual free surface conditions is lower than that in single free surface rockburst conditions. However, this energy is released more prominently near the peak stress. Therefore, when dual free surfaces are present, the area over which energy is released upon reaching the

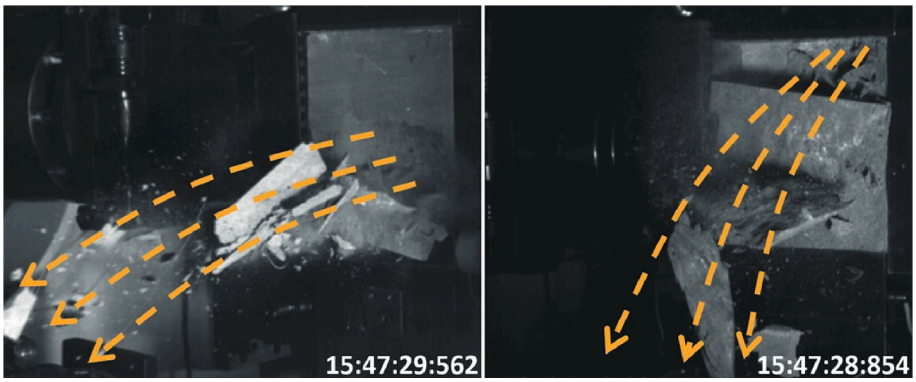

(a) Double free surface 1 (b) Double free surface 2

Fig. 3. Ejection characteristics of rockburst fragments from double free surfaces.

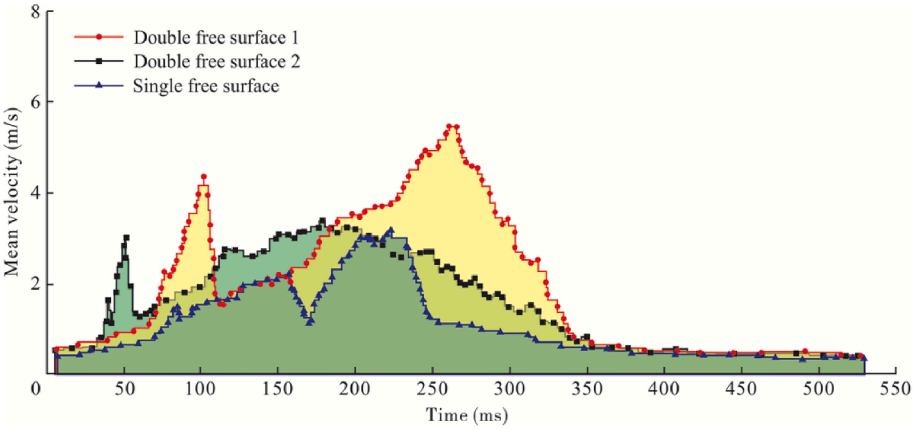

Fig. 4. Average ejection velocity of debris in two rockburst experiments.

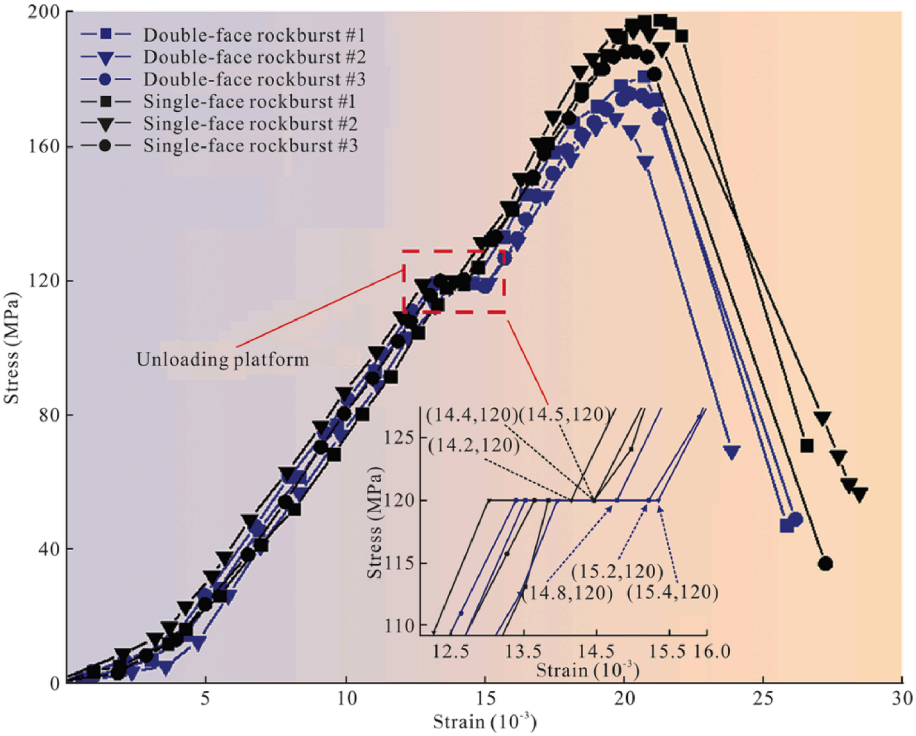

Fig. 5. Stress-strain curves of two rockburst experiments.

storage limit is larger than in single free surface scenarios, and the rate of energy release during a rockburst is higher. As a result, the rock is more prone to significant brittle failure and intense rockburst phenomena. High-speed camera footage of the rockburst damage indicates that dual free surfaces are more likely to trigger violent rockbursts and the unloading effect during the fast unloading is more pronounced.

3.3. AE characteristic evolution

3.3.1. AE events and AE location

AE, as a commonly used dynamic non-destructive testing technique, enables real-time and continuous monitoring of fracture locations during the rockburst incubation process in sandstone under external loading, and can determine the spatial coordinates of AE sources [17–19]. During the loading process, an AE event is recorded when the acoustic emission signal exceeds the acquisition threshold set in the experiment. Fig. 6 presents the time series characteristics of the AE count rate and cumulative AE counts for single-free-face and double-free-face rockburst specimens, respectively, under true triaxial loading and unloading conditions.

According to Fig. 6, the entire evolution process can be divided into three stages: (1) silent linear elastic deformation stage (Stage 1), (2) AE growth stage (Stage 2), and (3) AE-active rockburst stage (Stage 3). In Stage 1, both specimens exhibit a linear elastic response with very low AE event rates, while the AE event rate and cumulative count are slightly higher under double-face unloading conditions. At the moment of unloading, a brief AE pulse is observed in both cases; however, the sudden surge of AE events under double-face unloading is significantly greater than that under single-face unloading, indicating that double-face unloading under high confining pressure more easily triggers microcrack propagation. In Stage 2, the AE growth rate is higher for the double-face unloading specimen compared to the single-face one. In Stage 3, both the peak AE rate and the cumulative number of AE events under double-face unloading conditions are markedly higher than those observed under single-free-face rockburst. This comparison suggests that double-face rockburst not only initiates more microcrack activity at an earlier stage but also releases greater fracture energy in the subsequent stage, thereby accelerating and intensifying the rockburst process.

The localization of AE events enables the determination of damage and fracture locations, providing an effective means to investigate the dynamic evolution of microcrack initiation and propagation within rock specimens [20,21]. In this study, the spatial coordinates of AE sources

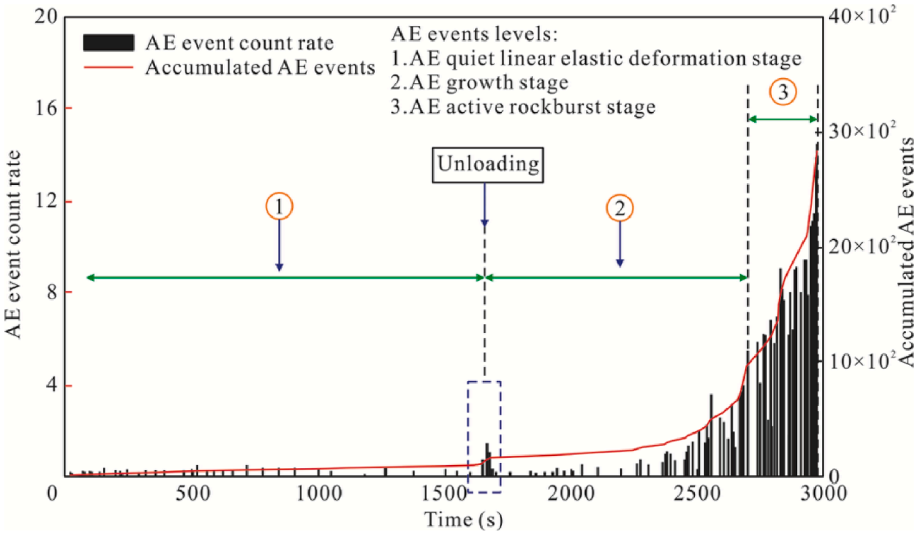

(a) Single free surface rockburst

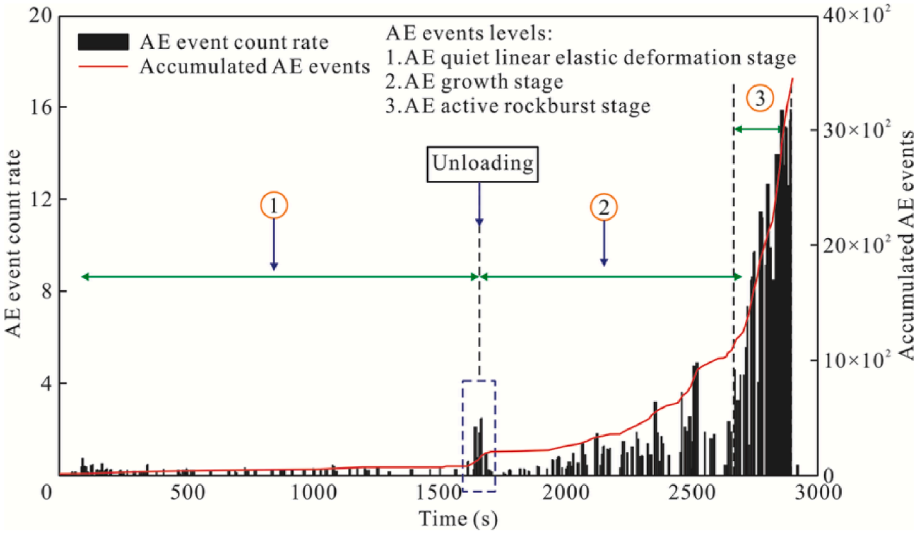

(b) Double free surface rockburst

Fig. 6. AE count rate-time curve.

were calculated based on the time-difference localization principle. By observing both the front and top views of the specimen after rockburst failure under double-free-face conditions (Fig. 7), the failure pattern can be roughly divided into two main parts: a single through-going crack on

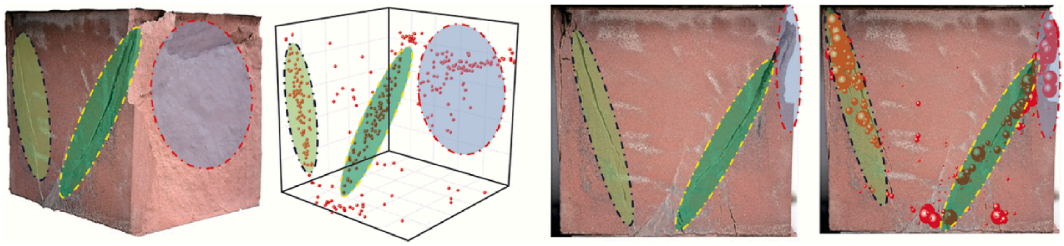

(a) Failure mode (b) AE event scatter plot (c) Side failure mode (d) Side AE event scatter plot

Fig. 7. AE event distribution of double free surface rockburst.

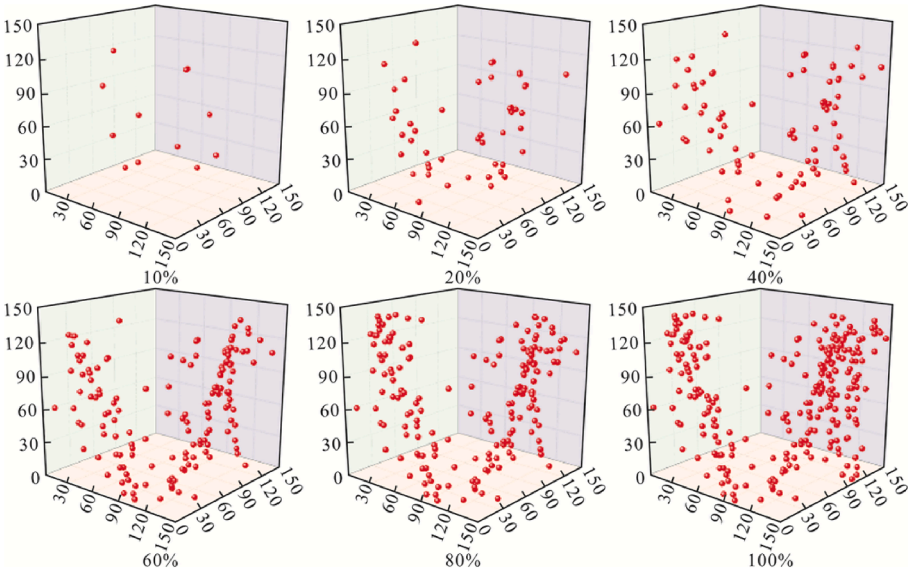

(a) Single free surface rockburst

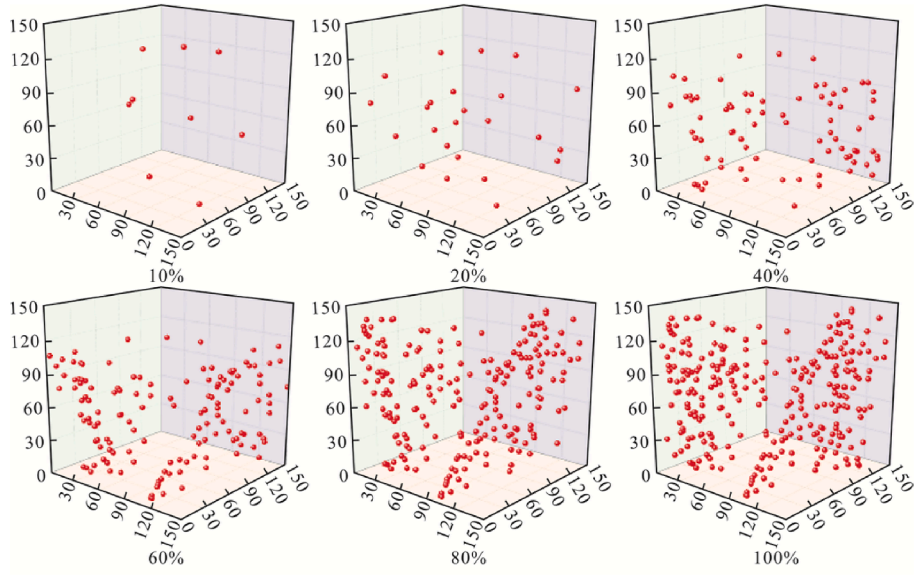

(b) Double free surface rockburst

Fig. 8. AE spatial localization segmented evolution diagram of two rockburst experiments.

the left side (highlighted by the yellow ellipse) and another on the right side (highlighted by the green ellipse). As shown in Fig. 7b, the AE events are densely distributed in the yellow and green regions corresponding to the observed cracks. Additionally, a cluster of AE events is also evident near the free surface of the specimen where failure occurred.

Based on the AE event localization evolution diagrams from the single free-face and double free-face rockburst experiments (Fig. 8), significant differences in the evolution processes between the two experimental conditions are observed. In the single free-face rockburst experiment, the evolution process is relatively straightforward. During the initial stage, AE events are sparse and scattered, primarily distributed near the free surface, indicating the initial formation of microcracks within the rock. As the experiment progresses, the number of AE events increases and begins to cluster near the free surface, suggesting crack propagation and stress concentration. Ultimately, at the moment of rockburst, AE activity surges sharply, forming a prominent cluster in the central part of the specimen.

In contrast, the evolution process in the double free-face rockburst experiment is more complex. Initially, AE events are also sparse but are distributed around both free surfaces, indicating simultaneous microcrack initiation near both boundaries. As the loading continues, AE events become concentrated around both free surfaces, reflecting bidirectional crack propagation and a more intricate stress field, accompanied by intensified AE activity. At the onset of rockburst, AE events peak near both free surfaces, resulting in two distinct clustering regions, indicative of more violent failure induced by the influence of the dual free surfaces. Comparative analysis reveals that AE events in the single free-face experiment are mainly concentrated near one free surface, with a more localized failure pattern. In contrast, AE events in the double free-face experiment are distributed near both free surfaces, showing a more dispersed failure mode and higher AE intensity. This difference is attributed to the more intense energy release caused by the presence of two free faces.

3.3.2. *AE crack evolution characteristics*

The spectral parameters of AE signals exhibit distinct characteristics corresponding to different types of microcrack formation [22]. AE signals with high average frequency (AF) and low rise time/amplitude ratio (RA) are typically associated with the initiation of tensile microcracks, whereas those with low AF and high RA values are indicative of shear microcrack formation [17]. In this study, AE signals recorded during the two types of rockburst experiments were analyzed to calculate their RA and AF values, from which RA–AF scatter plots were generated. Subsequently, K-medoids clustering analysis was performed [23–25], effectively classifying the AE events into two distinct groups [26]. K-medoids clustering is a classification method in the statistical field. It does not require the discriminant criteria to be known in advance. It can directly classify the original variables by the similarity between sample points, so it can be used for RA-AF association analysis. Fig. 9 presents the RA–AF scatter distributions of AE signals obtained from the single free-face and double free-face rockburst experiments in sandstone.

Based on the quantitative evolution patterns derived from the RA–AF distribution of acoustic emission (AE) signals, the types of microcracks were classified over time during the rockburst processes. For both types of rockburst experiments, the number of AE events corresponding to tensile and shear cracks was counted at regular time intervals, and the ratio of tensile to shear cracks was calculated accordingly. The results are presented in Fig. 10. The AE-derived crack evolution diagrams reveal significant differences in the crack development processes between the single free-face and double free-face rockburst experiments over the time interval of 0–3000 s. In the single free-face rockburst experiment, during the initial stage (0–1000 s), both tensile and shear cracks developed slowly, with event counts remaining below 200. In the middle stage, crack growth accelerated, with shear cracks exhibiting a steeper increase. In the later stage (1500–3000 s), shear cracks became dominant, ultimately reaching approximately 700, while tensile cracks peaked at around 400. In contrast, the double free-face rockburst experiment exhibited a more intense crack evolution. In the initial phase, both tensile and shear cracks increased slowly, but between 1000 and 1500 s, shear cracks accelerated markedly with a steeper growth slope. In the later stage (1500–3000 s), shear cracks continued to grow rapidly, ultimately approaching 900 events, while tensile cracks stabilized at approximately 500.

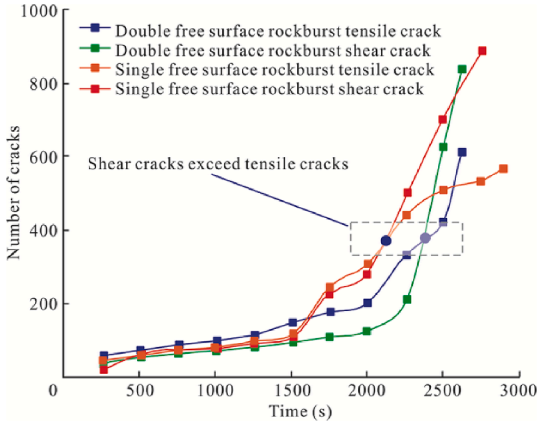

Fig. 10. Curves of the number of tension and shear cracks changing with time in two rockburst experiments.

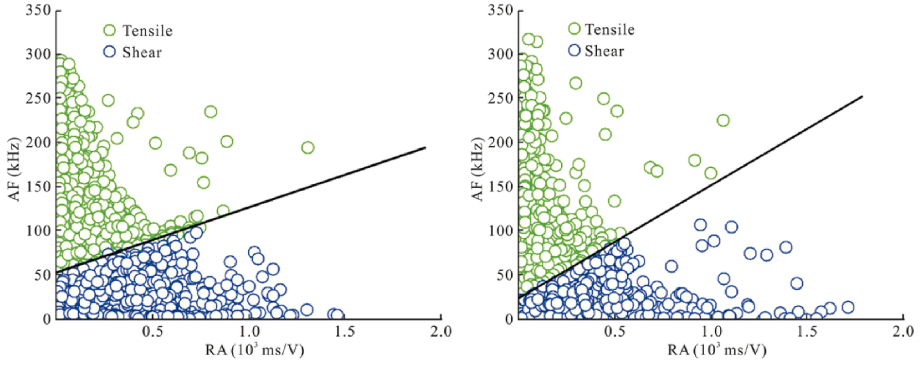

(a) Single free surface (b) Double free surface

Fig. 9. RA-AF distribution.

Comparative analysis indicates that the total number of cracks, particularly shear cracks in the double free-face experiment, was significantly higher than in the single free-face case. Moreover, in both experiments, the number of shear cracks exceeded that of tensile cracks during the 1500–2000 s interval. These results suggest that the presence of an additional free surface in the double free-face configuration enhanced crack propagation, especially accelerating the development of shear cracks, thereby leading to more severe damage. Conversely, the crack evolution in the single free-face experiment was more directional and gradual.

4. Conclusions

This study simulated rockbursts with dual free surfaces using a true triaxial experimental system. By comparing them with single free surface rockburst experiments, the evolution process and failure characteristics of dual free surface rockbursts were investigated. The main conclusions are as follows:

(1) Dual free surface rockbursts are more intense than single free surface rockbursts. The maximum ejection velocity of rock fragments in dual free surface rockbursts is 20 %–40 % higher than that in single free surface rockbursts. Moreover, the overall duration of ejection is longer. Due to the anisotropy of the rock, the ejection velocities from the two free surfaces differ.
(2) The peak stress of dual free surface rockbursts is lower than that of single free surface rockbursts due to reduced confining pressure. However, a more pronounced unloading plateau stage is observed during unloading. Compared with single-sided unloading, dual-sided unloading tends to cause more significant brittle failure and intense rockburst phenomena.
(3) Compared with single free surface rockbursts, dual free surface rockbursts induce more microcrack activity at an earlier stage and release higher rupture energy in the later stages. AE events in dual free surface experiments are mainly distributed near the two free surfaces, showing a more dispersed failure mode and higher activity intensity. The additional free surface in dual free surface rockbursts enhances crack propagation, especially shear cracks, leading to more severe sandstone damage after the rockburst.

CRediT authorship contribution statement

Jieyu Li: Writing – original draft, Writing – review & editing, Visualization, Investigation, Data curation. **Pengfei Shan:** Investigation, Visualization, Validation. **Jianning Liu:** Conceptualization, Methodology, Supervision, Project administration, Writing – review & editing. **Yunpeng Guo:** Methodology, Validation, Investigation. **Xiaomin Wang:** Data curation, Investigation. **Zihan Feng:** Visualization, Software, Investigation. **Chenguang Liu:** Investigation, Resources. **Chaochao Tian:** Validation, Formal analysis. **Yuting Mao:** Investigation, Data curation.

Declaration of competing interest

The authors declare the following financial interests/personal relationships which may be considered as potential competing interests: Zihan Feng is currently employed by Shuanglong Coal Mine, Huangling Mining, Shaanxi Coal Group, Chenguang Liu is currently employed by China Coal Technology Engineering Group Xi'an Research Insititute, and Chaochao Tian is currently employed by Ruineng Coal Mine, Huangling Mining, Shaanxi Coal Group. The other authors declare that they have no known competing financial interests or personal relationships that could have appeared to influence the work reported in this paper.

Acknowledgments

This work was supported by the State Key Laboratory for Tunnel Engineering (No. TESKL202424), National Natural Science Foundation of China (Nos. 52404142 and 52304111), and Yulin science and technology plan project of China (No. 2024-CXY-163).

References

[1] M. He, J. Li, D. Liu, K. Ling, F. Ren, A novel true triaxial apparatus for simulating strain bursts under high stress, Rock Mech. Rock Eng. 54 (2021) 759–775.
[2] Y. Pan, A. Wang, Disturbance response instability theory of rock bursts in coal mines and its application, Geohazard Mech. 1 (1) (2023) 1–17.
[3] N.G.W. Cook, The basic mechanics of rockbursts, J. S. Afr. Inst. Min. Metall 64 (3) (1963) 71–81.
[4] J. Deng, Y. Gong, S. Li, Induced mechanism of tunnel rockbursts based on dynamic buckling of rock plates, Geohazard Mech. 3 (1) (2025) 15–27.
[5] J. Zhou, X. Li, H. Mitri, Evaluation method of rockburst: state-of-the-art literature review, Tunn. Undergr. Space Technol. 81 (2018) 632–659.
[6] M. He, J. Miao, J. Feng, Rock burst process of limestone and its acoustic emission characteristics under true-triaxial unloading conditions, Int. J. Rock Mech. Min. Sci. 47 (2) (2010) 286–298.
[7] J. Li, D. Liu, M. He, J. Yang, Excess energy characteristics of true triaxial multi-faceted rapid unloading rockburst, J. Cent. South Univ. 31 (5) (2024) 1671–1686.
[8] S. Akdag, M. Karakus, A. Taheri, et al., Effects of thermal damage on strain burst mechanism for brittle rocks under true-triaxial loading conditions, Rock Mech. Rock Eng. 51 (2018) 1657–1682.
[9] G. Su, Y. Shi, X. Feng, J. Jiang, J. Zhang, Q. Jiang, True-triaxial experimental study of the evolutionary features of the acoustic emissions and sounds of rockburst processes, Rock Mech. Rock Eng. 51 (2018) 375–389.
[10] C. Wang, C. Li, B. Zhou, L. Sun, Z. Bai, C. Zhu, G. Wang, Q. Sui, J. Song, Temperature response of coal fracture induced by three-dimensional stress field, Measurement 227 (2024) 114258.
[11] F. Ren, M. Karakus, G. Nguyen, T. Bruning, Effects of pressure relief holes on coal burst: insights from true-triaxial unloading tests, J. Rock Mech. Geotech. Eng. 16 (9) (2024) 3378–3394.
[12] D. Liu, Z. Zhang, J. Yang, Q. Sun, Z. Liu, J. Sun, Effect of borehole pressure relief on rockburst: insights from borehole cooperative deformation mechanism, Rock Mech. Rock Eng. 58 (2) (2025) 2295–2317.
[13] J. Li, D. Liu, M. He, Y. Guo, H. Wang, Experimental investigation of true triaxial unloading rockburst precursors based on critical slowing-down theory, Bull. Eng. Geol. Environ. 82 (3) (2023) 65.
[14] D. Liu, K. Gu, J. Sun, Y. Zhang, J. Yang, Experimental study on rockburst of sandstone with different bedding dip angles, Rock Mech. Rock Eng. 58 (2) (2025) 2273–2293.
[15] Y. Qian, C. Zhao, Z. Dong, J. Xing, J. Niu, B. Zhang, Study on the self-initiated catastrophe mechanism of strain rockburst: a laboratory experiment, Int. J. Rock Mech. Min. 193 (2025) 106184.
[16] H. Wang, D. Liu, W. Gong, L. Li, Dynamic analysis of granite rockburst based on the PIV technique, Int. J. Min. Sci. Technol. 25 (2) (2015) 275–283.
[17] K. Du, X. Luo, M. Liu, X. Liu, J. Zhou, Understanding the evolution mechanism and classification criteria of tensile-shear cracks in rock failure process from acoustic emission (AE) characteristics, Eng. Fract. Mech. 296 (2024) 109864.
[18] W. Zhang, Z. Qiu, W. Liu, B. Zhang, W. Guo, Study on the AE characteristics and energy evolution mechanism of sandstone with different aspect ratios under biaxial compression, Rock Mech. Rock Eng. 57 (11) (2024) 9019–9034.
[19] C. Wang, B. Zhou, C. Li, Z. Wen, Z. Bai, C. Zhu, L. Sun, X. Xue, P. Cao, Prediction and critical transition mechanism for granite fracture: insights from critical slowing down theory, J. Cent. South Univ. 31 (8) (2024) 2748–2764.
[20] G. Feng, Z. Wang, Z. Li, Y. Zhang, Q. Meng, J. Gao, S. Xue, X. Zhang, Experimental study on re-crushing behaviour of crushed limestone based on acoustic emission location method, nondestruct. Test, Eval 39 (7) (2024) 2015–2031.
[21] C. Wang, B. Wang, C. Li, L. Huang, L. Sun, X. Xue, P. Cao, Investigation of the spatial correlation of rock crack propagation based on graph theory, Rock Mech. Rock Eng. 56 (3) (2023) 1981–1993.
[22] Z. Chen, G. Zhang, R. He, Z. Tian, C. Fu, X. Jin, Acoustic emission analysis of crack type identification of corroded concrete columns under eccentric loading: a comparative analysis of RA-AF method and Gaussian mixture model, Case Stud. Constr. Mater. 18 (2023) e02021.
[23] E. Herman, K.E. Zsido, V. Fenyves, Cluster analysis with k-mean versus k-medoid in financial performance evaluation, Appl. Sci. 12 (16) (2022) 7985.
[24] M. Wang, J. Li, Z. Shi, H. Tan, J. Wang, K. Li, Acoustic emission and fracture characteristics of red sandstone after high-temperature treatment, Eng. Fract. Mech. 306 (2024) 110245.
[25] Z. Chen, P. Wang, F. Shi, Investigation of crack recognition and spatio-temporal evolution pattern in coal samples damage, Sci. Rep. 13 (1) (2023) 17961.
[26] L. Dai, X. Zhao, Y. Pan, H. Luo, Y. Gao, A. Wang, L. Ding, P. Li, Microseismic criterion for dynamic risk assessment and warning of roadway rockburst induced by coal mine seismicity, Eng. Geol. (2025) 108324.